AIP | The Journal of Chemical Physics

Vibrational energy transfer from highly excited anharmonic oscillators. Dependence on quantum state and interaction potential

David J. Nesbitt and James T. Hynes

Citation: The Journal of Chemical Physics **76**, 6002 (1982); doi: 10.1063/1.442954
View online: http://dx.doi.org/10.1063/1.442954
View Table of Contents: http://scitation.aip.org/content/aip/journal/jcp/76/12?ver=pdfcov
Published by the AIP Publishing

Articles you may be interested in

State-resolved collisional energy transfer in highly excited NO 2 . II. Vibrational energy transfer in the presence of strong chemical interaction
J. Chem. Phys. **110**, 1404 (1999); 10.1063/1.478015

Vibrational energy transfer from highly excited anharmonic oscillators: Quasiclassical Monte Carlo trajectory study of Br2–Ar and Br2–Br system
J. Chem. Phys. **82**, 4903 (1985); 10.1063/1.448662

Vibration–translation energy transfer in anharmonic diatomic molecules. II. The vibrational quantum-number dependence
J. Chem. Phys. **64**, 1498 (1976); 10.1063/1.432368

Vibrational Energy Transfer from Highly Excited Molecules
J. Chem. Phys. **53**, 275 (1970); 10.1063/1.1673775

Vibrational Energy Exchange of Highly Excited Anharmonic Oscillators
J. Chem. Phys. **40**, 1289 (1964); 10.1063/1.1725311

This article is copyrighted as indicated in the article. Reuse of AIP content is subject to the terms at: http://scitation.aip.org/termsconditions. Downloaded to IP: 35.8.11.3 On: Thu, 28 Jan 2016 10:16:35

Vibrational energy transfer from highly excited anharmonic oscillators. Dependence on quantum state and interaction potential[a)]

David J. Nesbitt and James T. Hynes

Department of Chemistry, University of Colorado, Boulder, Colorado 80309
(Received 4 August 1981; accepted 9 March 1982)

In order to elucidate the general features of vibrational deactivation of highly excited anharmonic oscillators, we present quasiclassical trajectory calculations on prototype collinear I_2 (v)-inert gas collision systems. The results for vibrational-translational energy transfer reveal several interesting trends as a function of initial vibrational quantum state, projectile mass, and projectile–oscillator interaction potential. (1) Vibrational deactivation is inefficient from *all* quantum levels and for all projectile masses. The average energy transfer per collision ΔE is strongly peaked at intermediate vibrational levels ($v \approx 80$) and is observed to be at most $\approx -k_b T$. Further, when scaled to $\hbar\omega(E)$, the "local" oscillator energy spacing, ΔE can be accurately represented by a simple power law in vibrational quantum number over a wide range of bound states. (2) Energy transfer is progressively *less* efficient from levels in the neighborhood of and approaching dissociation. (3) Vibrational energy loss for high levels of initial vibrational excitation ($v > 90$) is rather insensitive to the nature of the interaction potential. Smooth exponential and hard-sphere interaction results differ by less than an order of magnitude. This observed insensitivity motivates the development of an analytic collision model, in which simple hard-sphere geometry and dynamics are used to calculate ΔE. The model results are in qualitatively good agreement with trajectory calculations and also indicate that nonuniform sampling of the anharmonic oscillator velocity and phase are responsible for decreased energy transfer efficiency from high vibrational states.

I. INTRODUCTION

In this paper, we present trajectory and analytic model studies of collisional energy transfer from highly vibrationally excited anharmonic oscillators.

Vibrational energy and its collisional transfer in both gas and liquid phases have received much attention in recent years.[1,2] The reasons for this scrutiny are readily appreciated. Vibrational excitation can be extremely important in surmounting activation barriers in simple chemical systems; indeed, orders of magnitude rate enhancement per quantum have been reported.[3] Similarly, vibrational deactivation processes are crucial in stabilizing intermediate species once they have crossed an activation barrier.[4] Vibrational energy transfer phenomena, therefore, can strongly influence the overall dynamics of product formation in chemical reactions.

There is presently a wealth of experimental and theoretical information available on low-lying vibrational states, i.e., $v = 1, 2$. Deactivation rates and energy transfer cross sections have been measured for a large number of singly vibrationally excited molecules.[5] Theoretical efforts to develop models that correctly predict empirical trends in the experimental data have been reasonably successful.[1,2,6,7] Direct overtone excitation with tunable visible and near infrared lasers has been used to study vibrational deactivation in several small molecules with a few quanta of excitation.[8]

In contrast to the abundance of data and theoretical perspective on singly excited levels, there is relatively little known about higher vibrational states. (A few notable exceptions will be mentioned below.) A fundamental barrier to detailed experimental investigation is the difficulty of cleanly producing populations in high lying individual vibrational levels of the ground electronic state. Successive overtone transitions occur with rapidly diminishing oscillator strength; this seriously limits potential extension of direct overtone excitation techniques to higher vibrational levels. An alternative approach exploits the fact that exothermic gas phase chemical reactions can readily generate products in high vibrational states. However, a broad population of several quantum levels often results.[9] Similar difficulties arise using rapid fluorescence from electronically excited states to populate high levels in the ground state; appreciable Franck–Condon factors typically extend over many vibrational transitions.[10] Quantitative measurement of vibrational deactivation rates from such broad, initial distributions necessitates deconvoluting the time dependence of all the levels. This considerable task has been performed in only a few diatomic systems, most notably HF($v \leq 7$),[8(e),(g)] HCl($v \leq 7$),[8(g)] and CO($4 \leq v \leq 12$).[9(c)] Vibrational deactivation in *excited* electronic states of I_2 has been probed successfully by laser induced fluorescence methods in an extensive set of studies by Steinfeld and co-workers.[11] Preparation and monitoring of specific high vibrational levels in the *ground* electronic state of I_2 by stimulated emission pumping[12] and other double resonance techniques promise invaluable insight into relaxation phenomena of highly excited species.

Theoretical attention to vibrational relaxation of highly excited anharmonic oscillators has been largely

a)Supported in part by a grant from the National Science Foundation.

 0021-9606/82/126002-13$02.10 © 1982 American Institute of Physics

This article is copyrighted as indicated in the article. Reuse of AIP content is subject to the terms at: http://scitation.aip.org/termsconditions. Downloaded to IP: 35.8.11.3 On: Thu, 28 Jan 2016 10:16:35

confined to the immediate neighborhood of dissociation. The focus on this region is due to the considerable interest in dissociation–recombination reactions. Only a few trajectory studies have spanned a large range of vibrational levels, notably studies of Br_2 at 1500 K in He, Ar, and Xe by Clarke and Burns,[13] and of the excited electronic B state of I_2 in the rare gases by Rubinson, Garetz, and Steinfeld.[14] We are aware of only one attempt, due to Mahan,[15] at an analytic model treatment of collisional energy transfer to and from excited anharmonic oscillators over a wide vibrational energy range. This treatment has been generalized somewhat by Rubinson *et al.* for comparison with their I_2 B-state trajectory results.[14] Unfortunately, this analytic model predicts qualitatively incorrect trends (*vide infra*) over most of the vibrational levels of an anharmonic oscillator.

Despite the considerable difficulty noted above in cleanly investigating highly vibrationally excited species, much of gas and liquid phase chemistry depends heavily upon them. For example, a complete understanding of unimolecular processes requires a detailed knowledge of vibrational activation and deactivation rates.[16] Atom recombination dynamics hinge on the ability of a third body to stabilize the newly formed and highly internally excited molecule.[17] Even chemical reactions in the liquid phase require vibrational quenching of the nascent product to prevent reverse motion across an activation barrier.[4,18]

The purpose of this paper is to investigate the nature of vibrational deactivation from highly excited states in an anharmonic oscillator as a function of several key system parameters: (i) vibrational quantum state, (ii) projectile mass, and (iii) collisional interaction potential. To elucidate the general features of these trends, we present both the results of extensive numerical trajectory calculations as well as of a simple analytic model. The latter is based on a highly approximate hard sphere interaction picture which permits clear physical interpretation of the collisional dynamics. Despite its simplicity, the model exhibits surprisingly good qualitative agreement with the trajectory studies. It should be stressed that our primary interest in this work is in generating an initial basis for further quantitative investigation; we aim to develop an intuition on vibrational deactivation phenomena in an important regime where experimental data are difficult to obtain and relevant theory is lacking.

The organization of this paper is as follows. In Sec. II, we review the background assumptions and mathematical details used in the trajectory calculations. In Sec. III, the observed energy transfer dependence on oscillator quantum state and oscillator-projectile interaction potential is presented. In Sec. IV, we introduce a hard sphere model in an effort to illuminate the fundamental trends in the trajectory studies on a simple physical level. The model's strengths and weaknesses, as well as further directions for quantitative refinement, are briefly discussed. The broad implications of these deactivation studies are considered in Sec. V.

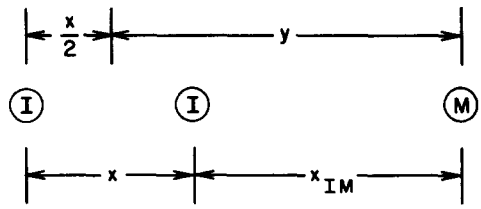

FIG. 1. Definition diagram for the collinear I_2–M energy transfer.

II. TRAJECTORY CALCULATIONS

In this paper, we will take the collinear I_2-inert gas system as our prototypical model of vibration-translation energy transfer. In this section, we discuss this model and the details of the trajectory calculations of the energy transfer.

A. Model assumptions

It has long been recognized that the marginal extra accuracy afforded by exhaustive quantum mechanical calculation is simply not warranted for describing ground state nuclear motion for many heavy atom systems of practical interest.[19] This would seem to be also true for the I_2-inert gas systems. The de Broglie wavelength of the projectile at room temperature is substantially smaller than the physical dimensions of the collision interaction. The vibrational spacing in I_2 for low lying states is ~ 220 cm^{-1},[20] i.e., roughly k_bT at room temperature; this spacing gradually decreases to small fractions of k_bT as one approaches the dissociation limit. We therefore follow standard quasiclassical techniques for monitoring the collision dynamics, i.e., we use classical trajectories but quantized initial oscillator energies.[14]

Throughout this paper the collinear collision geometry of Fig. 1 will be employed. The I_2 oscillator is bound in a nonlinear Morse potential

$$V_{osc} = D\{1 - \exp[-\beta(x - x_e)]\}^2, \tag{2.1}$$

with dissociation energy $D = 60.1487\ k_bT$ at $T = 300$ K, equilibrium I–I separation $x_e = 2.6668$ Å, and $\beta^{-1} = 0.5229$ Å.[21] There are 114 bound vibrational levels for this potential. The collinear collision partner, a structureless inert gas atom, interacts with the oscillator via an exponential repulsion

$$V_{int} = D_i \exp(-\alpha x_{IM}). \tag{2.2}$$

Here x_{IM} is the separation of atom M and the nearest oscillator I atom. Parameters for V_{int} were initially taken as $D_i = D$ and $\alpha = 2\beta$. This corresponds to taking the M–I repulsion as analogous to the repulsive part of the I–I potential. In order to investigate systematically interaction potential effects on energy transfer efficiency, we have also considered a range of α values from this somewhat "soft" value 2β, up to an essentially "hard-sphere" value 256β.

The ability of a collinear collision geometry such as ours to reproduce accurately the dynamic characteristics of a full three-dimensional interaction has been extensively discussed for low vibrational levels.[22]

This article is copyrighted as indicated in the article. Reuse of AIP content is subject to the terms at: http://scitation.aip.org/termsconditions. Downloaded to IP: 35.8.11.3 On: Thu, 28 Jan 2016 10:16:35

TABLE I. Ratio R of vibrational to rotational frequencies for I_2, Eq. (2.3), as a function of vibrational energy and quantum level.

E/D	0.0	0.1	0.3	0.5	0.9	0.99	0.999
v	0	6	19	33	78	102	110
R	39.5	37.7	33.6	28.9	13.9	4.84	1.67

Quantitative comparison between exact numerical and analytic solutions for low vibrational states indicates the critical parameter to be the ratio of vibrational spacing ω_e to the rotational spacing $2B_eJ$. This ratio gauges the difference in characteristic frequencies for vibration and rotation. If $\omega_e/2B_eJ \gg 1$, results of a collinear geometry, suitably averaged over effective impact parameters, are then in excellent agreement with full three-dimensional solutions.[22] For high vibrational states, however, this ratio must be generalized to include oscillator energy-dependent frequencies, whereby the anharmonicity and bond length distortion of the oscillator are taken explicitly into account. The Morse oscillator frequency $\omega(E)$ as a function of energy can be readily derived. A conservative estimate of $B(E)$, the energy-dependent rotational constant, can be calculated from an average of the inner and outer turning point displacements. Typical J values are estimated from equipartition. This leads to a ratio

$$R = \frac{\omega(E)}{2B(E)J} \approx \frac{\omega(E)}{2[B(E)k_bT]^{1/2}} = \left[\frac{\beta^2(D-E)I}{\mu_{osc}k_bT}\right]^{1/2} , \quad (2.3)$$

where μ_{osc} is the oscillator reduced mass, and where the effective moment of inertia is given by

$$I(E) = \mu_{osc}\{x_e - (4\beta)^{-1}\ln[1 - E/D]\}^2. \quad (2.4)$$

For I_2, R is well above unity for energies up to about 99% of the dissociation limit (see Table I). Thus the collinear model is expected to represent the collision dynamics quite adequately over most of the I_2 vibrational levels. Nevertheless the one-dimensional model will break down very near the dissociation limit, where the vibrational and rotational frequencies approach each other. In addition, the presence of rotational barriers is important in three dimensional collision dynamics near dissociation. In fact, Burns and co-workers[13] have indicated that vibration-rotation transfer is important near dissociation. Except in the unlikely event of very high angular momentum, however, the influence of this vibration-rotation coupling should fall rapidly as the immediate vicinity of the dissociation threshold is left.

B. Trajectory calculation details

Here we outline the details of the trajectory calculations of I_2–M vibrational energy transfer over the entire range of I_2 vibrational energy levels.

As described above, the I_2 oscillator is governed by an anharmonic Morse potential and interacts collinearly with a projectile via the adjacent I atom according to $V_{int}(x_{IM})$. The system Hamiltonian is (cf. Fig. 1)

$$H = \tfrac{1}{2}\mu_{osc}\dot{x}^2 + \tfrac{1}{2}\mu_M\dot{y}^2 + V_{osc}(x) + V_{int}(y - \gamma x), \quad (2.5)$$

where the cyclic center-of-mass coordinate has been eliminated, and in which the oscillator and projectile reduced masses are

$$\mu_{osc} = \frac{m_I}{2} \; ; \quad \mu_M = \frac{2m_Im_M}{2m_I + m_M} . \quad (2.6)$$

The I–M separation x_{IM} has been expressed in terms of the oscillator relative coordinate x, the coordinate y of M relative to the oscillator center of mass, and the mass factor $\gamma = m_I/2m_I = 1/2$.

Oscillator intial conditions were chosen from an analytic algorithm for uniformly sampling the vibrational phase:

$$x^{init} = \beta^{-1}\ln\left\{\frac{1 - (E/D)^{1/2}\sin[2\pi k/(k_{max}+1)]}{1 - E/D}\right\} + x_e \; ;$$
$$k = 1, 2, \ldots, k_{max} . \quad (2.7)$$

The projectile was released from a fixed starting point sufficiently far from the most extended oscillator turning point to prevent interaction effects at the initial time $t=0$. The initial relative projectile velocity v_0 was selected by an algorithm for uniform sampling of an appropriate Maxwellian room temperature 300 K velocity distribution. The velocities were chosen to satisfy

$$\int_0^{v_0(i)} dv' P_{Maxwell}(v') = \frac{i}{i_{max}+1} , \quad (2.8)$$

for $i = 1, 2, 3, \ldots, i_{max}$. The appropriate velocity distribution to use for $P_{Maxwell}$ is not entirely clear in connection with any ultimate conversion from a one-dimensional model to the three-dimensional world.[1(a),1(c),1(f)] Here we use the three-dimensional flux distribution (taking $v_0 > 0$ for collision)

$$P_{Maxwell} = \left(\int_0^\infty dv_0 v_0^3 \exp(-\mu_M v_0^2/2k_bT)\right)^{-1} \times v_0^3 \exp(-\mu_M v_0^2/2k_bT) . \quad (2.9)$$

Twenty phases of the oscillator, each at ten projectile velocities, were sampled for every ten vibrational states from $v=0$ to $v=110$; there are thus 200 trajectories for every v value. A variable step size Runge–Kutta integration program[23] was used on a PDP 11/40 system to integrate Hamilton's equations. Trajectories were followed until the projectile was again outside the range of the interaction potential; the change in vibrational energy was then calculated. Energy conservation served as a guide to the numerical accuracy of the trajectories, and was consistently better than 99.99%.

III. TRAJECTORY CALCULATION RESULTS

In this section, we present the calculated vibrational energy transfer as a function of (a) the initial I_2 oscillator vibrational state and (b) the character of the iodine-collision partner interaction potential. Vibrational energy transfer is also investigated as a function of projectile mass, i.e., masses corresponding to inert gas family members. For simplicity in discussion, we focus primarily on the $I_2(v)$–Ar system, and refer to interesting mass trends where appropriate.

This article is copyrighted as indicated in the article. Reuse of AIP content is subject to the terms at: http://scitation.aip.org/termsconditions. Downloaded to IP: 35.8.11.3 On: Thu, 28 Jan 2016 10:16:35

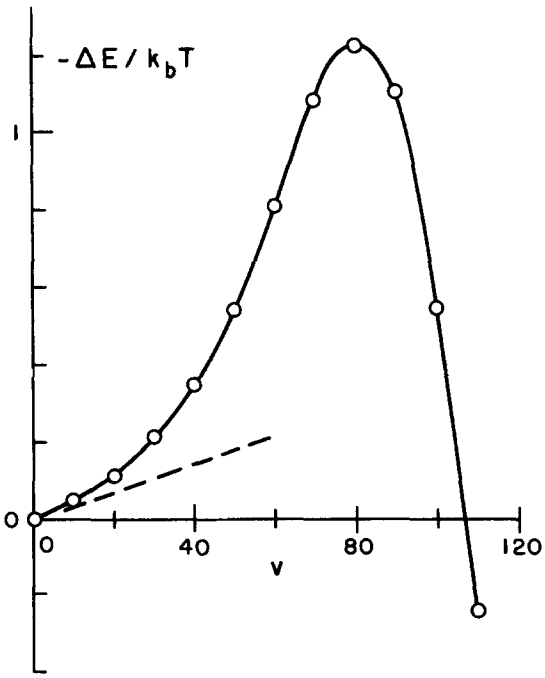

FIG. 2. Phase and velocity averaged vibrational energy transfer for the I_2–Ar system as a function of initial I_2 vibrational level v. Dashed line is an extrapolated LT-type linear v dependence. As $v \to 0$, ΔE becomes slightly positive.

A. Quantum state dependence

The full trajectory results on energy transfer in the $I_2(v)$–Ar prototype system as a function of oscillator quantum state v are displayed in Fig. 2. Several interesting and even startling features are immediately evident.

(1) The energy transfer is *not* a monotonic function of quantum number v; rather, a distinct maximum appears around $v = 80$. This indicates that energy transfer, though initially scaling with vibrational state for low levels, eventually becomes *less* efficient as one progresses up the vibrational ladder. We stress that this turnover is not due to the onset of large positive energy changes in individual dissociative collisions. At $v = 90$ for example, more than $2k_bT$ transfer is required for dissociation; we observed such transfer in only $\approx 2\%$ of the trajectories.

(2) Even at the optimal vibrational state, energy transfer is surprisingly *inefficient*, given the amount of vibrational energy in the oscillator: approximately 1.2 k_bT is lost per collision. For vibrational levels away from this peak, the energy transfer drops off precipitously, approaching minute fractions of $-k_bT$.

Two important points should be stressed at this stage. First, the small observed average energy changes are *not* the result of nearly cancelling gains and losses of large amounts of energy in individual collisions. Energy changes of $O(k_bT)$ or less are the norm (Fig. 3). Second, even small energy changes near the top of the well correspond to significant changes in the vibrational quantum number. Note, for example, that the vibrational spacing at $v = 80$, 90, and 100 is about $k_bT/3$, $k_bT/5$, and $k_bT/8$, respectively.

We pause to note that such energy transfer could be called efficient in a certain sense. For example, $\Delta E = 0(-k_bT)$ for high closely spaced levels indicates that a vibrational transition occurs on nearly every collision. From the perspective of the very small transition probabilities obtained for low v levels (Fig. 2), this is efficient energy transfer. We term energy transfer of order k_bT or less inefficient in the sense that such ΔE values are a very small fraction of the large vibrational energy potentially available for collisional transfer.

(3) At vibrational levels very near the dissociation limit, ΔE turns positive; dissociation in a collision is highly probable. At $v = 80$, no dissociation is observed. At $v = 90$, about 2% of the trajectories lead to dissociation; this climbs rapidly to $\approx 80\%$ at $v = 110$.

Some partial results closely related to our own have also been found by, or are implicit in results of, pre-

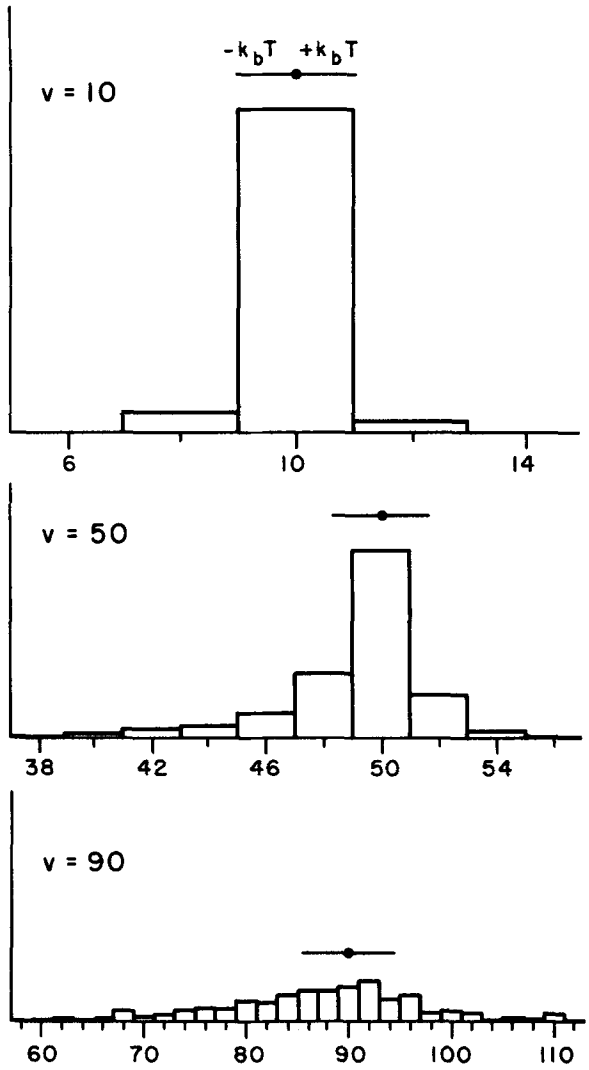

FIG. 3. Details of I_2–Ar vibrational energy transfer patterns. Shown are trajectory histograms for given initial levels v; sorting is by every two vibrational levels. The measure of k_bT is also shown.

This article is copyrighted as indicated in the article. Reuse of AIP content is subject to the terms at: http://scitation.aip.org/termsconditions. Downloaded to IP: 35.8.11.3 On: Thu, 28 Jan 2016 10:16:35

TABLE II. Summary of energy transfer results for $I_2(v)$–inert gas systems.[a]

	$-\Delta E/k_bT$		$-\Delta E_{max}$		% Dissociated		
	$v=10$	$v=100$	k_bT	${}^v\Delta E_{max}$	$v=90$	$v=100$	$v=110$
He	2.67×10^{-1}	5.06×10^{-1}	0.96	60	0.5	7.0	53.5
Ne	1.14×10^{-1}	5.51×10^{-1}	1.46	70	1.0	20.0	70.5
Ar	4.13×10^{-2}	5.40×10^{-1}	1.22	80	1.5	22.5	75.5
Kr	2.92×10^{-3}	3.67×10^{-1}	0.73	90	1.0	23.0	79.5
Xe	5.81×10^{-4}	2.24×10^{-1}	0.44	90	0.0	23.0	82.0

[a]For these trajectory results, the I_2–M repulsion was characterized by $\alpha=2\beta$. Therefore the inert gas collision partner labels refer solely to different collision partner mass and not to different interaction potential.

vious investigators. First, there is a suggestion of the nonmonotonic dependence of energy transfer efficiency in Br_2–He calculations of Clarke and Burns[13(a)] and in experimental results of Steinfeld and Schweid[24] on the electronically excited B state of I_2. Second, the inefficiency of energy transfer in the near neighborhood of dissociation has been found by Benson and Berend[25] for a one-dimensional model of I_2 collisions, and by Keck[17(b)] in several three-dimensional computer studies. The inefficient character of energy transfer for intermediate to high levels can be inferred from three-dimensional computational results of Clarke and Burns[13(a)] for high temperature relaxation of Br_2, and of Rubinson *et al.*[14] for relaxation of the B state of I_2. Finally, the strong onset of probability of dissociation near the threshold has been seen in a number of calculations of Burns and co-workers.[13]

We have also performed $I_2(v)$–M energy transfer trajectory calculations for projectiles corresponding to the inert gas masses, with α held fixed at $\alpha=2\beta$. The results, listed in abbreviated form in Table II, indicate several features worth noting. (1) Energy transfer from low vibrational levels is very sensitive to projectile mass, being 460 times more efficient for He than Xe at $v=10$. As we shall see, this trend is fully substantiated by the Landau–Teller theory,[7,8] and is due primarily to the higher thermal velocities of the lighter species. (2) At high vibrational levels, this sensitivity to mass and/or velocity is greatly attenuated; the results for the He and Xe masses differ by only a factor of 2.3 at $v=100$. The juxtaposition of these first two observations indicates that fundamentally different collision dynamics control energy transfer in these two regimes. (3) All projectile masses exhibit a maximum energy transfer. Peak energy transfer is most efficient for the Ne mass, and drops off somewhat for both lighter and heavier projectiles. The position of this peak occurs at systematically higher vibrational levels for the heavier masses. (4) Finally, the probability of dissociation from the highest level ($v=110$) increases monotonically with projectile mass.

1. Comparison with Landau-Teller theory

To place our observations in perspective, it is worth considering the qualitative predictions of the familiar Landau–Teller (LT) theory[6] for the $I_2(v)$–Ar system. While this theory has been superseded by much more sophisticated and numerically accurate treatments,[1] it still provides a useful guide to qualitative trends and important key parameters. The LT model is based on a *harmonic* oscillator that remains *fixed* in extension over the collision duration. These assumptions of course should break down severely for high v. The celebrated LT expression for collisional transition probability between adjacent levels is of the form[26(a)]

$$P(v\to v-1)\propto v\exp(-2\pi\omega/\alpha v_0)\ , \tag{3.1}$$

which leads to a linear dependence on v for ΔE.[26(b)] Here $\omega=2\pi\nu$ is the harmonic vibrational frequency, α characterizes the repulsive interaction potential $[\exp(-\alpha x_{IM})]$, and v_0 is the relative collision velocity.

The *qualitative* LT prediction of linear v dependence plotted in Fig. 2 coincides with the full trajectory results only for low-lying vibrational states. At higher levels of excitation, the trajectory calculations indicate qualitatively different behavior than the LT gradual, *linear* rise with quantum number. We conclude, to no one's surprise, that the LT linear v scaling is a poor guide to higher level energy transfer.

It is, however, instructive to note that the simple LT model fails not only by its prediction of a linear rise as a function of quantum state, but also by its extreme sensitivity to α, the "steepness" of the exponential wall[1(c)]; a mere doubling of α results in a virtually explosive increase in energy transfer efficiency. From a practical standpoint, this sensitivity to α can make quantitative *a priori* predictions of deactivation rates exceedingly difficult.[1(a)] In Sec. III B, we show that at intermediate to high quantum levels, the actual energy transfer efficiency in fact becomes far less critically dependent on the repulsive potential slope.

2. Power law dependence

The trajectory results in Fig. 2 can be replotted to highlight an extremely surprising and promising trend. At the bottom of the I_2 well, vibrational states are nearly evenly spaced. As the dissociation limit is approached, however, this spacing monotonically decreases to zero. Consequently, a more appropriate measure of the prob-

This article is copyrighted as indicated in the article. Reuse of AIP content is subject to the terms at: http://scitation.aip.org/termsconditions. Downloaded to IP: 35.8.11.3 On: Thu, 28 Jan 2016 10:16:35

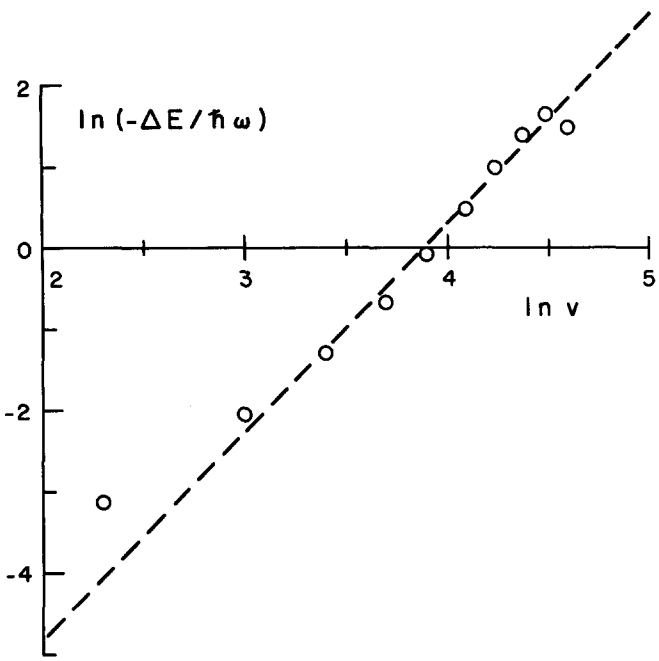

FIG. 4. Log–log plot of $-\Delta E/\hbar\omega(E)$, the average energy loss for the I_2–Ar system divided by the local vibrational energy spacing, vs vibrational quantum number. The line is least squares fit between $v=20$ and 90 and has slope 2.54.

ability of a collisional change in vibrational level would be $\Delta E/\hbar\omega(E)$, i.e., the energy transfer divided by the energy separation of adjacent quantum states.[27(a)] A log–log plot of $\Delta E/\hbar\omega(E)$ vs v is shown in Fig. 4. This plot is fairly linear, particularly up to near the dissociation limit. Thus, *energy transfer scaled to the "local", i.e., energy-dependent, frequency is accurately predicted by a power law in vibrational quantum number*

$$-\Delta E/\hbar\omega(E)=Av^n\,. \tag{3.2}$$

The startling aspect of this result is that the power law dependence is exhibited for such a simple model system over such a wide range of vibrational states. We have verified this trend also for each of the inert gas projectile masses[27(a)] as well as for a wide range of interaction potentials, from soft ($\alpha=2\beta$) to hard sphere ($\alpha=256\beta$). The results are summarized in Table III. It is worth noting two features: (1) Best fit exponent values are very sensitive to projectile mass for soft collision potentials, whereas for hard sphere potentials, the dependence on projectile mass is greatly reduced. (2) Best fit exponents for $\alpha=256\beta$ interaction potentials are nearly unity, i.e., $\Delta E/\hbar\omega(E)$ varies approximately linearly with v for hard spheres. In Sec. IV, we present analytic solutions for simple hard-sphere collision models which correctly predict this linear dependence.

Relevant experimental data for comparison on deactivation of highly excited anharmonic oscillators from a progression of quantum states are scarce. However, studies on V–T, R self-relaxation of HF(v) and DF(v) indicate that the rates do indeed scale as a power law in vibrational quantum number.[28] However, HF has many non-V–T relaxation channels in such processes and is also decidedly more quantum mechanical than $I_2(v)$–Ar. We therefore cannot claim these HF data as illustration of our results. Nevertheless, our trajectory data suggest an exciting possibility: energy transfer rates measured low in the vibrational well might be extrapolated with acceptable accuracy up to experimentally inaccessible states close to the dissociation limit.[27(b)] Theoretical efforts to elucidate this intriguing trend and its generality are presently under way; some initial results are presented in Sec. IV.

B. Interaction potential dependence

It is well established that energy transfer for low vibrational states is dominated by the strong repulsive forces experienced at small internuclear separations.[1] Indeed, the LT Eq. (3.1) identifies a key "adiabaticity" parameter

$$A=2\pi\omega/\alpha v_0 \tag{3.3}$$

as a rough measure of overall energy transfer efficiency. If the collision duration [$\propto(\alpha v_0)^{-1}$] is very small compared to the oscillator period ($\propto\omega^{-1}$), then $A\ll 1$ and energy transfer is efficient in this impulsive, *nonadiabatic* regime. Conversely, when $A\gg 1$, the *adiabatic* regime is reached and energy transfer is markedly inefficient ($\propto e^{-A}$ according to LT theory).

The harmonic frequency for I_2 is $\omega=4.2\times10^{13}$ s^{-1} and $\alpha=2\beta=3.82$ Å^{-1} in our model. If we use the most important contributing thermal speed[1] $v_0=(2\pi\omega k_bT/\alpha\mu_M)^{1/3}\approx 7.5\times10^4$ cm s^{-1}, then

$$A\approx 8.6 \tag{3.4}$$

for the I_2–Ar system. It is thus clear that, despite the fact that the I_2 level spacing is comparable to k_bT at 300 K, the I_2–Ar system lies well in the adiabatic regime for low levels. As a result, the energy transfer should be extremely sensitive to interaction potential curvature at low v (as in the LT theory). It is not immediately clear, however, that this generalization is valid for intermediate to high vibrational levels. We have therefore investigated energy transfer in the $I_2(v)$–Ar system for various forms of the collision interaction. The exponential potential ($V_{int}=D\exp(-\alpha x_{IM})$) was continuously varied from a soft ($\alpha=2\beta$) to a virtually hard sphere interaction ($\alpha=256\beta$). The results of these calculations

TABLE III. Best fit exponents to the power law expression for vibrational energy transfer: $-\Delta E/\hbar\omega(E)=Av^n$.

	n	
M	$\alpha=2\beta$[a]	$\alpha=256\beta$
He	1.11	0.995
Ne	1.92	0.960
Ar	2.54	0.908
Kr	3.62	0.809
Xe	4.30	0.741

[a]The results for $\alpha=2\beta$ have been previously published in Ref. 27(a).

This article is copyrighted as indicated in the article. Reuse of AIP content is subject to the terms at: http://scitation.aip.org/termsconditions. Downloaded to IP: 35.8.11.3 On: Thu, 28 Jan 2016 10:16:35

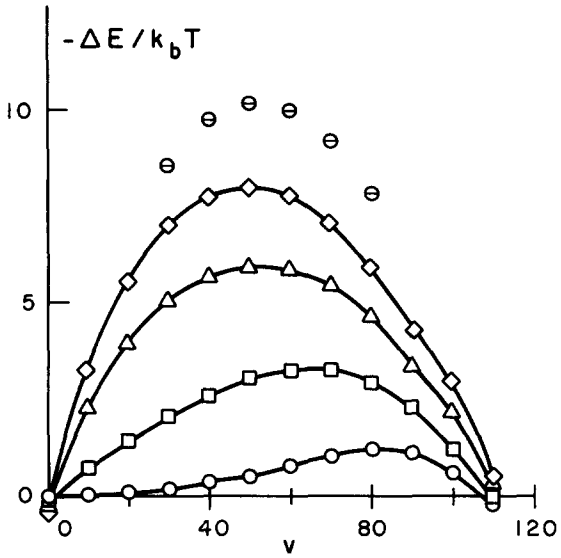

FIG. 5. Vibrational energy transfer as a function of steepness of the I_2–M interaction potential Eq. (2.2) vs vibrational level. Legend: 0, $\alpha = 2\beta$; □, $\alpha = 4\beta$; △, $\alpha = 8\beta$; ◇, $\alpha = 16\beta$; θ, $\alpha = 256\beta$. Here the projectile mass is that of Ar, $m_M = 39.9$.

are presented in Fig. 5 and can be briefly summarized.

(1) The *qualitative* trends in the trajectory data are similar for all values of α: energy transfer is most efficient for intermediate vibrational levels and drops off steeply to either side of this maximum.

(2) Vibrational deactivation efficiency grows monotonically with α. At intermediate and high vibrational levels, this trend of ΔE with α is *in disagreement* with that of the analytic model treatment of Mahan[15] for this regime.[14] For low vibrational levels, energy transfer is acutely sensitive to α. This is in agreement with the simple Landau–Teller picture, which suggests an exponential α dependence. [See Eq. (3.1).]

(3) At intermediate levels, ΔE is *still* sensitive to α, but in a less pronounced fashion. Evidently energy transfer is still significantly removed from the nonadiabatic limit.

(4) At high levels of excitation, however, the sensitivity to α is decidedly decreased. For $v \gtrsim 90$, energy transfer differs by less than factors of 4 over the range $\alpha = 2\beta$ to $\alpha = 256\beta$.

IV. ANALYTIC MODEL FOR ENERGY TRANSFER

A rather subtle picture of anharmonic oscillator energy transfer has emerged from our trajectory calculations. For all quantum states, energy transfer is inefficient. As we proceed from low to intermediate levels, the average energy transfer rises. For high quantum states v, vibrational deactivation decreases dramatically (Fig. 2); this is a qualitatively different trend than that predicted by harmonic, perturbative treatments, e.g., Landau–Teller. In addition, the sensitivity of this high-v deactivation to the interaction potential is far less than exponential (Fig. 5). To generate physical insight into the underlying dynamics of these trends, we present an analytic collision model based on hard sphere interactions and straightforward geometric arguments. All comparisons with trajectory data are made with the $I_2(v)$–Ar system.

A. Hard sphere model description

The fundamental physical bases of our hard sphere model are two. First, for very highly vibrationally excited states, an anharmonic oscillator spends the majority of the time far out on the slowly varying, attractive limb of the Morse potential. There it moves at substantially lower velocities than when close in over the well. This is reflected in the average kinetic energy plot in Fig. 6. Over the duration of the collision therefore, the oscillator experiences a relatively small acceleration from the binding potential. Consequently, it is reasonable to expect that for these collisions, the overall energy transfer dynamics ought to resemble those of *unbound* particles. We thus propose that the dynamics can be calculated to a first approximation from a hard sphere, impulsive picture. For given oscillator and projectile velocities then, we will use the well-known hard sphere result for energy transfer.[29]

Secondly, in this hard sphere limit, the projectile velocities reduce to straight line segments, with finite discontinuities in the first derivative at the collision points. Hence, the regions of oscillator phase that are accessed by the projectile can be determined from simple geometric considerations.

We anticipate, and will later find, that the quantitative accuracy of these assumptions will be best for high

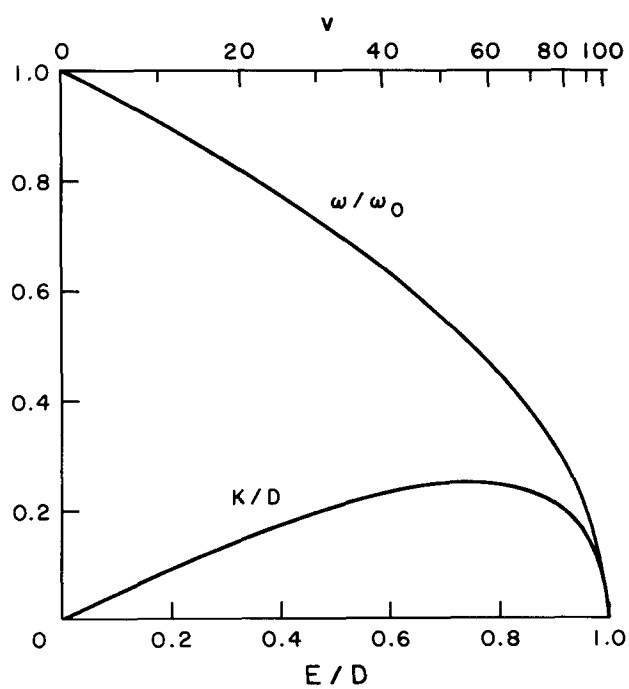

FIG. 6. Vibrational energy and quantum level dependence of I_2 Morse oscillator characteristics. Here $\omega(E)/\omega_0$ is the oscillator frequency reduced by its low energy harmonic value. The average oscillator kinetic energy $\bar{K}$ is reduced by the dissociation energy D. Note that since $D = 60\, k_b T$, the maximum phase averaged kinetic energy is $\approx 15\, k_b T$.

This article is copyrighted as indicated in the article. Reuse of AIP content is subject to the terms at: http://scitation.aip.org/termsconditions. Downloaded to IP: 35.8.11.3 On: Thu, 28 Jan 2016 10:16:35

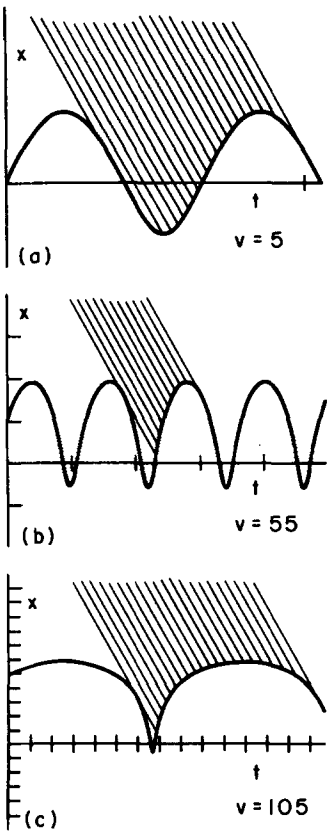

FIG. 7. Illumination of the I_2 anharmonic oscillator by collision partner (Ar) trajectories for various quantum levels v. See the text. The position and time axes are marked (in 0.5 a.u. and harmonic period units, respectively) to show the relative scales for different vibrational states.

lying levels. This is already clear from Fig. 5 where for $v \geq 90$ the energy transfer is not sensitively dependent upon the stiffness of the interaction potential. We will nonetheless employ them for all levels. We now exploit these considerations in constructing our model.

1. Role of the oscillator phase

The displacement versus time of the anharmonic oscillator motion is portrayed as a periodic series of asymmetric bumps in Fig. 7. At high vibrational energies, these bumps become dramatically skewed to the lower velocity regions near the outer turning point. The projectile motion in the hard sphere limit is represented by a family of oblique lines angling downward onto these bumps; the first point of intersection marks a collision. This perspective was first introduced by Benson, Berend, and Wu,[30] who developed a hard sphere model for collisional energy transfer from *harmonic* oscillators. Here we develop the hard sphere model to predict and understand the collisional energy transfer from *anharmonic* oscillators.

As might be expected, the "density" of projectile-oscillator collisions is highest near the turning point, for there the oscillator is moving most slowly. For certain regions of vibrational phase, however, the oscillator is receding from the projectile with a greater velocity than that of the projectile. Trajectories of this nature result in a collision only *after* the oscillator has reached its inner turning point and hurtles outward once more. Consequently, not all phases of the oscillator are sampled, and even for those that are, the phases are sampled with different probabilities. In order to average over all possible collisions, therefore, we need only consider the regions of anharmonic oscillator motion that are "illuminated" by the parallel "rays" corresponding to a uniform distribution of projectile phases. We can simply focus on the intensity of the projectile's illumination, so to speak, over the physically accessible, and hence illuminated, regions of oscillator phase. Such optical terminology will often prove convenient in what follows.

2. Qualitative trends

These rather simple considerations generate two unambiguous predictions for energy transfer.

(1) In the hard sphere limit, energy loss is determined by the *kinetic* rather than by total energy of the oscillator.[29] The average kinetic energy of the oscillator increases with quantum level for $v \lesssim 60$ (Fig. 6); hence one should expect rapidly increasing energy transfer efficiency as a function of vibrational state. As v increases further, however, this increase is slowed by the following effect. The regions of phase where the oscillator is moving rapidly tend to be in the "shadow" of the skewed anharmonic oscillator trajectories [Figs. 7(a) and 7(b)]; therefore, collisions tend to sample a distribution of somewhat *lower* kinetic energies.[20] Consequently, we have two opposing trends, and the predicted general increase in energy transfer from intermediate vibrational states is somewhat impeded.

(2) As the oscillator is elevated to even higher vibrational states ($v > 90$), the fraction of time spent in the low velocity regions described above increases [Fig. 7(c)]. This is also reflected in the dropping average oscillator kinetic energy (Fig. 6). One then predicts an eventual *decrease* in energy transfer as a function of vibrational quantum number.

These predictions are exceptionally well borne out by the trajectory calculations of Sec. III (Fig. 2). Evidently the key dynamical features of the full trajectory studies are embodied in this simple, hard sphere model. We are therefore emboldened to present its full analytic solution.

B. Analytic solution

The solution of the hard sphere model involves four basic steps. First, the range of illuminated oscillator phases, i.e., those accessible in a collision, is established. Second, the probability distribution for those collisions which are allowed is constructed. Third, energy transfer for such collisions is calculated. Finally, combination of the above in an appropriate average gives the average energy transfer.

We must first calculate the dividing boundaries between the shaded and illuminated regions of phase. These are labeled (x_1, t_1) and (x_2, t_2) in Fig. 8 (we set x_e to zero for convenience). To find these, we first

This article is copyrighted as indicated in the article. Reuse of AIP content is subject to the terms at: http://scitation.aip.org/termsconditions. Downloaded to IP: 35.8.11.3 On: Thu, 28 Jan 2016 10:16:35

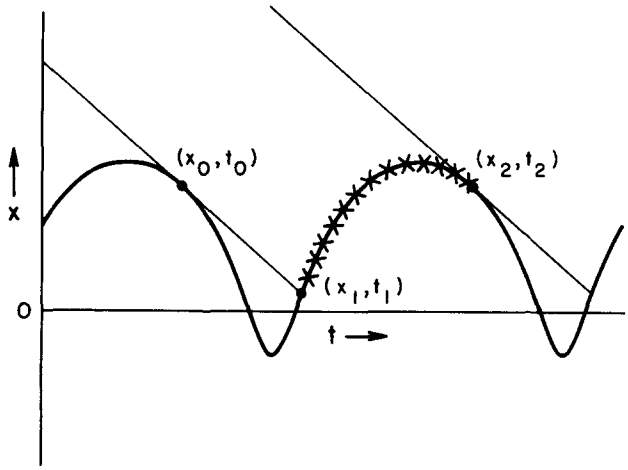

FIG. 8. Definition diagram for the hard sphere model. See the text.

examine the point (x_0, t_0) in Fig. 8. This is obviously related to the desired outer boundary by

$$x_2 = x_0 \; ; \quad t_2 = t_0 + T \; , \tag{4.1}$$

where T is the oscillator period

$$T = 2\pi/\omega(E) = (2\pi/\beta)(\mu_{osc}/2(D-E))^{1/2} \; . \tag{4.2}$$

At (x_0, t_0), the oscillator and projectile velocities match, i.e., the displacement versus time trajectories are parallel. For an incident relative projectile velocity $v_0 = \dot{y}$, this occurs at

$$x_2 = x_0 = -\beta^{-1} \ln[1 - \sqrt{(E - 2\mu_{osc} v_0^2)/D}] \tag{4.3}$$

at a time $t_0 = t_2 - T$ given by

$$\omega(E) t_0 = \sin^{-1}((D/E)^{1/2}[1 - (1 - E/D)\exp(\beta x_0)]) \; . \tag{4.4}$$

Here we have used the known solutions to the Morse oscillator equations of motion.[31] Note that both x_2 and $t_2 = t_0 + T$ depend upon the incident relative projectile velocity v_0.

The outer phase boundary (x_2, t_2) is now established. The inner boundary (x_1, t_1) can be found from Fig. 8 by solving

$$x_0 - v_0(t_1 - t_0) = \beta^{-1} \ln\left(\frac{1 - (E/D)^{1/2} \sin \omega(E) t_1}{1 - (E/D)}\right) \tag{4.5}$$

for t_1, noting Eq. (4.1), and then calculating

$$x_1 = \beta^{-1} \ln\left(\frac{1 - (E/D)^{1/2} \sin \omega(E) t_1}{1 - (E/D)}\right) \; . \tag{4.6}$$

Regrettably, Eq. (4.5) is transcendental and can only be analytically solved in certain limits. Here we choose to maintain generality and solve Eq. (4.5) for t_1 numerically. We proceed, then, assuming that t_1 is known.

Our next step is to construct the probability $P(v_{osc}, v_0)$ that a collision occurs. Oscillator phases between (x_0, t_0) and (x_1, t_1) are inaccessible to the projectile. Collisions can only occur in the illuminated region where the oscillator phase lies within (x_1, t_1) to (x_2, t_2). For v_{osc} outside this region, $P(v_{osc}, v_0)$ is identically zero. Inside this region, $P(v_{osc}, v_0)$ can be shown by simple geometry to be

$$P(v_{osc}, v_0) = \left[\int_{t_1}^{t_2} dt \left(v_0 - \frac{v_{osc}}{2}\right)\right]^{-1} \left(v_0 - \frac{v_{osc}}{2}\right) \; , \tag{4.7}$$

i.e., proportional to the *relative* velocity of oscillator and projectile.[32,33]

We next need to calculate the energy transfer in the hard sphere limit for each time t in the interval (t_1, t_2). This is a standard problem in elementary classical mechanics, with the minor complication that the reduced oscillator particle can have both translational and internal excitation. For collision velocities v_{osc} and $v_0 = \dot{y}_0$, the change in vibrational excitation of the oscillator is[29]

$$\Delta E(v_{osc}, v_0) = \frac{m_I}{(m_I + m_M)^2}\left[\frac{m_I v_{osc}}{2} + m_M v_0\right]^2 - \frac{m_I v_{osc}^2}{4} \; . \tag{4.8}$$

Note that this solution is defined only for $v_{osc} \leq 2v_0$, i.e., when the collision actually occurs.

We now have the illuminated phase region, the collision probability in that region, and the energy transfer in a collision. The oscillator phase average energy transfer in the hard sphere model is then

$$\Delta E(v_0) = \int_{t_1}^{t_2} dt \, P(v_{osc}, v_0) \, \Delta E(v_{osc}, v_0) \; . \tag{4.9}$$

Substitution of Eqs. (4.7) and (4.8) into Eq. (4.9) yields a series of integrals of Morse oscillator velocities raised to various powers:

$$I_n = \int_{t_1}^{t_2} dt [v_{osc}(t)/2]^n \; ; \tag{4.10}$$

these are discussed in Appendix A. One finds that

$$\Delta E(v_0) = m_I m_M (m_I + m_M)^{-2} A_0^{-1} \times [m_M v_0^2 A_0 + 2m_I v_0 A_1 - (m_M + 2m_I) A_2] \; , \tag{4.11}$$

where $A_i = v_0 I_i - I_{i+1}$. The I_n depend upon v_0 through the limits t_1 and t_2.

The final hard sphere model result for the fully averaged oscillator vibrational energy transfer is just the Maxwellian flux average of this [cf. Eq. (2.9)],

$$\Delta E \equiv \int dv_0 \, P_{Maxwell}(v_0) \, \Delta E(v_0) \; , \tag{4.12}$$

which can be integrated numerically.

C. Hard sphere model results

Equation (4.12) for the averaged energy transfer was evaluated for the $I_2(v)$–Ar prototype system as a function of vibrational quantum state; the results are presented in Fig. 9.

The important features can be briefly summarized. (1) The hard sphere model generally overestimates the energy transfer for all vibrational states, but is in reasonable agreement with the trajectory data for the higher quantum levels. (2) The trajectory calculations for progressively higher values of the repulsive force curvature α converge to the results of the hard sphere model. This is of significant practical importance; the computer time associated with generating the model results is virtually negligible compared with the full trajectory studies.

This article is copyrighted as indicated in the article. Reuse of AIP content is subject to the terms at: http://scitation.aip.org/termsconditions. Downloaded to IP: 35.8.11.3 On: Thu, 28 Jan 2016 10:16:35

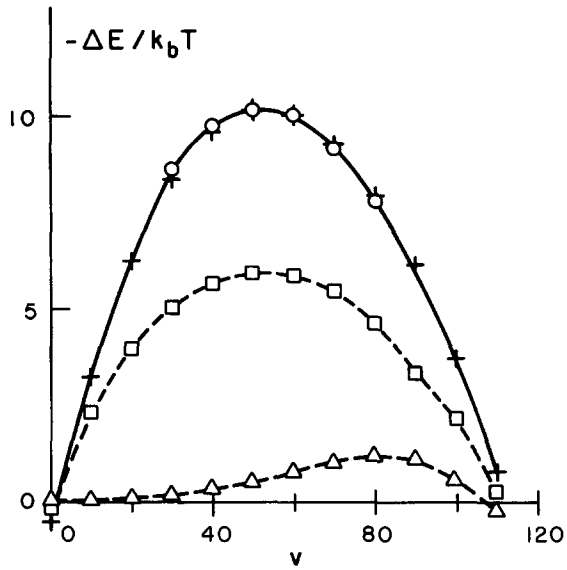

FIG. 9. Test of the hard sphere model predictions (+) for energy transfer. Circles represent trajectory data for $\alpha = 256\beta$. Shown for comparison are the trajectory data for $\alpha = 2\beta(\Delta)$ and $\alpha = 8\beta(\square)$. It is a failing of the model that average energy transfer to the oscillator is not predicted at the very highest levels (Appendix B).

But of greater relevance is the purely qualitative success of the hard sphere model, i.e., the correct prediction of an initial rise in energy transfer efficiency as v increases through low and intermediate values, and especially the prediction of a decrease in energy transfer efficiency at high vibrational levels. The corresponding gross trends in the full trajectory calculations can therefore be interpreted in terms of the simple physical framework of the model (cf. Figs. 6 and 7) as follows.

Low in the well, the average speed of the I_2 oscillator is on the order of thermal velocities (Fig. 6). Consequently, all phases of the oscillator are sampled; energy transfer is limited primarily by the small average kinetic energies involved and deactivation is inefficient.

Higher in the well, the average oscillator speed is superthermal (Fig. 6) and energy transfer rises steeply as a distribution of high relative velocities is sampled. Illumination of all oscillator phases by the projectile trajectories is however, partially constrained [Fig. 7(b)]: some shadowed, inaccessible phases occur when the oscillator has high kinetic energy. Thus the rise of energy transfer is somewhat slowed.

For *very high* vibrational states in the well, however, the anharmonic oscillator spends most of the time hovering near the outer turning point [Fig. 7(c)]. As a result, the majority of the collisions occur at near thermal velocities (Fig. 6), and as at the bottom of the well, energy loss is severely impeded.

In summary, the hard sphere model provides a simple and instructive framework for the interpretation of all the important trends in the computer generated energy transfer results.

D. Simplifications of the hard sphere model

Many of the qualitative characteristics of vibrational energy transfer in highly anharmonic oscillators are successfully predicted by the hard sphere model. The features that are responsible for this success can be best isolated by considering two simplifications. The hard sphere mechanics dictate that the collisional oscillator energy transfer is $\Delta E(v_{osc}, v_0)$ given by Eq. (4.8). The two simplifications we consider deal with the calculation of the phase average energy transfer $\Delta E(v_0)$. Equation (4.9) shows that this average involves (i) the influence of the relative collision velocity $v - \frac{1}{2}v_{osc}$ through the probability $P(v_{osc}, v_0)$, Eq. (4.7), and (ii) the effects of the restricted phase (t_1, t_2).

In the first simplified treatment, we ignore both the relative velocity effect $P(v_{osc}, v_0)$ and the phase restrictions, i.e., we set $t_1 = 0$ and $t_2 = T$ (cf. Fig. 8). In this simple phase average (SPA), integrals over terms linear in v_{osc} vanish, while integrals over quadratic terms in v_{osc} can be related to the fully phase averaged oscillator kinetic energy $\overline{K}$. The result is

$$\Delta E(v_0)\big|_{SPA} = -\frac{m_M(m_M+2m_I)}{(m_I+m_M)^2}\,\overline{K} + \frac{m_I m_M^2}{(m_I+m_M)^2}\,v_0^2 . \tag{4.13}$$

The subsequent Maxwellian average of this gives the average energy transfer as

$$\Delta E_{SPA} = -\frac{m_M(m_M+2m_I)}{(m_I+m_M)^2}\,(\overline{K} - 2k_bT) , \tag{4.14}$$

which explicitly links the oscillator energy loss to its average kinetic energy.

In the second simplified treatment, we continue to ignore the phase restrictions, and set $t_1 = 0$ and $t_2 = T$. Now, however, we retain the relative velocity factor $P(v_{osc}, v_0)$ in the weighting of collision probability. In this approximate relative velocity average approximation (RVA), the integrals I_n, Eq. (4.10), over a full oscillator period vanish for odd n and we are left with

$$\Delta E(v_0)\big|_{RVA} = \frac{m_I m_M^2 v_0^2}{(m_I+m_M)^2} - \frac{m_M(m_M+4m_I)}{(m_M+m_I)^2}\,\overline{K} . \tag{4.15}$$

A subsequent average over the Maxwellian distribution of projectile relative velocities gives

$$\Delta E_{RVA} = -\frac{m_M(m_M+2m_I)}{(m_I+m_M)^2}\,(\overline{K} - 2k_bT) - \frac{2m_M m_I}{(m_I+m_M)^2}\,\overline{K} , \tag{4.16}$$

i.e., the same result as the simple phase average approximation, but with an extra loss term proportional to the average oscillator kinetic energy.

Figure 10 displays the predictions of the hard sphere model and its two simplifications as a function of quantum level. The average oscillator kinetic energy is included for purposes of comparison. There are several interesting features. (1) The correlation between the predictions and $\overline{K}$ is clearly apparent. This is entirely reasonable in the hard sphere regime: a fixed fraction of the kinetic energy is transferred per collision, and

This article is copyrighted as indicated in the article. Reuse of AIP content is subject to the terms at: http://scitation.aip.org/termsconditions. Downloaded to IP: 35.8.11.3 On: Thu, 28 Jan 2016 10:16:35

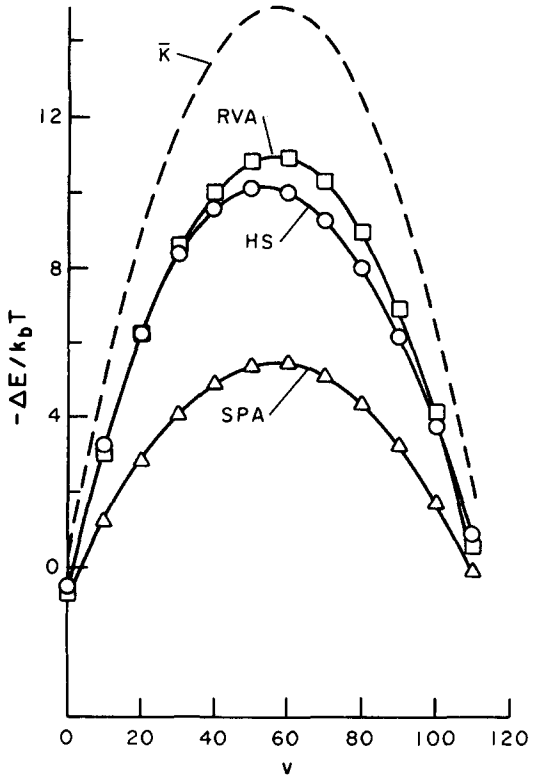

FIG. 10. Comparison of the Hard Sphere (HS) Model and its approximations. Note that the relative velocity average approximation predicts energy transfer values that are within 20% of the full hard sphere model values.

is strictly a function of the mass coupling. (2) The dependence upon $\bar{K}$ is independent of the form of the oscillator potential. For a purely harmonic potential, for example, $\bar{K}$ would increase linearly with quantum number, and so would the predicted energy transfer. This permits us to assign unambiguously the decrease in energy transfer efficiency at high levels in both model and trajectory studies to effects of an *anharmonic* oscillator potential. (3) The relative velocity average approximation predicts a consistently more efficient energy transfer than the simple phase average approximation. This is a direct consequence of weighting more favorably the high relative velocity encounters; by Eq. (4.8) this costs dearly in oscillator kinetic energy in a collision. (4) Results of the relative velocity average approximation are in rather good agreement with the full hard sphere model results. This strongly indicates that inclusion of relative velocity in weighting collision probability is much more important than considering incomplete illumination of oscillator phase.

We now have fully analytic solutions for energy transfer from highly excited anharmonic oscillators in the hard sphere limit. It would be interesting to see if the surprising power law dependence results of Table III can be predicted *a priori*. For each of the approximations to the hard sphere model, energy transfer varies linearly with the average kinetic energy $\bar{K}$ of the oscillator

$$\bar{K}=\frac{1}{T}\int_0^T dt\,\tfrac{1}{2}\mu_{osc}v_{osc}^2(t)\ . \tag{4.17}$$

This can be related to the vibrational level v. We first convert Eq. (4.17) to an integral over the full roundtrip displacement of the oscillator via $dt=dx/v_{osc}(x)$:

$$\bar{K}=\frac{1}{2T}\oint dx[\mu_{osc}v_{osc}(x)]\ . \tag{4.18}$$

The integral in Eq. (4.18) is the action (i.e., $\oint p\,dx$) of the vibrational motion, and is equal to $\hbar(v+1/2)$.[34] Since the period T is $2\pi/\omega(E)$, we obtain the simple result

$$\bar{K}=\hbar\omega(E)(v+1/2)/2\ , \tag{4.19}$$

which is valid for *any* form of the oscillator potential. For low v, this reduces to the familiar harmonic virial theorem result.

From the approximate hard sphere model results then, energy transfer is dominated by the average kinetic energy, which in turn varies linearly with the "*local*" oscillator vibrational spacing, $\hbar\omega(E)$. The ratio of $-\Delta E/\hbar\omega(E)$ therefore will vary approximately as

$$-\Delta E/\hbar\omega(E)\propto\frac{\bar{K}}{\hbar\omega(E)}=\tfrac{1}{2}(v+1/2)\ . \tag{4.20}$$

Equation (4.20) predicts that energy transfer in these simple approximate hard sphere models, scaled to the vibrational energy spacing, will depend linearly on v (for $v\gg 1$). This is exceptionally well substantiated by the power law fits to hard sphere energy transfer shown in Table III. Although the power law in these analytic treatments is simply a proportionality, the predictive success at the hard sphere level offers hope for a more complete understanding of the power law behavior for softer collision interactions.

E. Adiabaticity effects

The impressive *qualitative* success of the hard sphere model notwithstanding, it is important to understand the origin of its decidedly less dazzling *quantitative* performance (Fig. 9). The model clearly overestimates energy transfer efficiency. The major difficulty appears to be the neglect of adiabaticity effects in our impulsive, nonadiabatic model. As discussed in Sec. III A, the low quantum level energy transfer is strongly adiabatic; the adiabaticity parameter $A=2\pi\omega/\alpha v_0$ [Eq. (3.3)] is large [Eq. (3.4)]. Figures 5 and 9 show that this problem, while muted, remains for intermediate and higher levels. Actually, this is not so surprising when it is realized that the anharmonic Morse oscillator frequency (Fig. 6) is still fully one half of the harmonic value at $E/D=0.75$ ($v=60$).

At the highest levels, the low energy adiabaticity parameter A must be replaced by a high energy parameter which gauges the influence of the oscillator displacement during a collision; this is carried out in Appendix B. We conclude there that adiabatic, finite duration of collision effects decrease as dissociation is approached but are still not entirely negligible (Figs. 5 and 9).

Our results suggest that the hard sphere model should be modified to account explicitly for finite collision time adiabatic effects to generate a more nearly *quantitative* description of excited oscillator energy transfer. We leave this for future attention.

This article is copyrighted as indicated in the article. Reuse of AIP content is subject to the terms at: http://scitation.aip.org/termsconditions. Downloaded to IP: 35.8.11.3 On: Thu, 28 Jan 2016 10:16:35

V. SUMMARY AND DISCUSSION

The results of this study indicate several interesting and unexpected conclusions.

(1) Vibrational energy transfer for highly excited oscillators is inefficient on the scale of the oscillator vibrational energy. Maximum energy transfer for the $I_2(v)$–Ar system, which occurs at fairly high levels of vibrational excitation ($v \simeq 80$), is only about $-k_bT$, and drops off sharply in magnitude for higher and lower levels. This overall feeble character is at first glance quite surprising: the vibrational energy itself exceeds $10\ k_bT$ for $v \geq 10$. The inefficiency of the energy transfer involves two basic features. First, the I_2–Ar system is in the adiabatic regime. Second, accessible phase considerations tend to bias the oscillator kinetic energy toward lower values; less kinetic energy K is available for transfer. Note that it is only K, and not E, that can be transferred in an impulsive collision. Thus, for example, a "strong collision assumption," in which all the vibrational energy is transferred in a collision, is nowhere valid.

(2) Energy transfer from oscillators very near dissociation is highly inefficient on the scale of the oscillator vibrational energy. The major cause of inefficient energy transfer from high vibrational levels is the distinctly nonuniform sampling of oscillator velocity and phase, especially the former. As the quantum state approaches the dissociation limit, most collisions take place near the outer turning point, and hence, occur predominantly at slow, energy-deficient oscillator velocities. This important point was noted as well by Benson and co-workers.[25,30] This can have considerable implications for the stabilization of newly formed molecular species in a chemical reaction or atom—atom recombination processes. Lifetimes of loosely bound nascent oscillators may be substantial, and processes competing with stabilization may become very important.

(3) The ratio of energy transfer to local vibrational level spacing can be accurately characterized by a simple power law in v over a wide range of vibrational states. This astonishingly simple result may provide an extrapolation method for reasonably accurate deactivation rates of high vibrational levels presently inaccessible to experiment.

(4) The good agreement at high levels of excitation between full trajectory calculations and predictions of the hard sphere model offers hope for approximate numerical validity of similar models in very anharmonic systems. Our discussion of the hard sphere model assumptions indicates that (a) energy transfer inefficiency at high vibrational levels reflects the decrease in average oscillator kinetic energy and (b) that a more nearly quantitative description of energy transfer may result by inclusion of the effects of a finite collision duration.

The purpose of this work has been to expose several interesting and important vibrational deactivation phenomena for highly excited anharmonic oscillators. We have made several fundamentally simple observations which provide a useful conceptual and semiquantitative guide through these phenomena. Our success at this level suggests that a more comprehensive theoretical framework for energy transfer dynamics can be developed.

In subsequent papers we will examine mass and velocity effects on anharmonic oscillator energy transfer[35] and the possible role of slow vibrational relaxation in liquid state picosecond recombination experiments.[36]

ACKNOWLEDGMENTS

The authors wish to express their gratitude to Dr. Judah Levine for his generous offer of computer time on the PDP 11/40 system, as well as for frequent advice on implementing software. Professor F. F. Crim is gratefully acknowledged for bringing the early work of Benson and co-workers to our attention.

APPENDIX A

The integrals I_n, Eq. (4.10), of powers of the Morse oscillator velocity are simply related to the (indefinite) integrals

$$K_n = \int dt(1 - a\sin t)^{-n}\cos^n t\ , \tag{A1}$$

with $0 \leq a \leq 1$. For $n = 0$, integration is trivial. For $n = 1$, the integrand is a perfect differential and

$$aK_1 = -\ln(1 - a\sin t)\ . \tag{A2}$$

For $n = 2$ and 3, the substitution $z^{-1} = 1 - a\sin t$ reduces the K_n (with some labor) to known integrals.[37] One finds that

$$a^2K_2 = [(a^2-1)z^2 + 2z - 1]^{1/2} - \sin^{-1}[(az)^{-1}(z-1)] - (1-a^2)^{-1/2}\sin^{-1}\{a^{-1}[(a^2-1)z^2+1]\}\ ; \tag{A3}$$

$$2za^3K_3 = (a^2-1)z^3 + 4z^2 - 2z\ln z\ . \tag{A4}$$

APPENDIX B

For high vibrational states, we can couch the duration of collision problem of Sec. IV E in the following physical terms. If the spatial domain of the collision corresponds to significant variation in the oscillator potential, then an impulsive approximation can be poor: the vibrational kinetic energy K of the oscillator is changed as much or more by the oscillator potential than by the projectile potential. As a numerical guide, we can define a high energy adiabaticity parameter

$$\zeta \equiv \left| \frac{\frac{\partial V_{osc}}{\partial x}(\Delta x)_{osc}}{K} \right|_{coll} \tag{B1}$$

suitably averaged over all possible collisions. For $\zeta \gg 1$, a collision occurs over large changes in the binding potential, and energy transfer cannot be simply predicted from the hard sphere Eq. (4.9). Conversely, for $\zeta \ll 1$, the collision takes place over small changes in the binding potential, and thus energy transfer can be adequately calculated from a hard sphere picture.

For highly excited anharmonic oscillators, ζ can be estimated with a few approximations. Most collisions occur near the outer turning point, at roughly thermal velocities. We therefore approximate K by k_bT, Δx_{osc} by $v_{osc}(v_0\alpha)^{-1}$, $\partial V_{osc}/\partial x$ by its turning point value, and

This article is copyrighted as indicated in the article. Reuse of AIP content is subject to the terms at: http://scitation.aip.org/termsconditions. Downloaded to IP: 35.8.11.3 On: Thu, 28 Jan 2016 10:16:35

take v_{osc} and v_0 to be their thermal values. This yields

$$\zeta = \frac{2\beta D(E/D)^{1/2}[1-(E/D)^{1/2}]}{(k_b T)(\mu_{osc}/\mu_0)^{1/2}\alpha} . \quad \text{(B2)}$$

For $E/D = 0.8$ ($v \approx 65$) and $\alpha = 2\beta$, ζ can be readily calculated to be ≈ 4; this is certainly far from the nonadiabatic regime, $\zeta \ll 1$. In fact only for $E/D \gtrsim 0.95$ is ζ even less than unity! In other words, for all but the very highest vibrational levels (i.e., $E/D \approx 1$), the finite duration of the oscillator-projectile collision still significantly influences energy transfer dynamics (Figs. 5 and 9). This suggests that the hard sphere model should be modified to take into account explicitly the local binding potential slope.

[1](a) D. Rapp and T. Kassal, Chem. Rev. 69, 61 (1969); (b) T. L. Cottrell and C. McCoubrey, *Molecular Energy Transfer in Gases* (Butterworths, London, 1961); (c) J. T. Yardley, *Introduction to Molecular Energy Transfer* (Academic, New York, 1980); (d) H. K. Shin, in *Dynamics of Molecular Collisions, Part A*, edited by W. H. Miller (Plenum, New York, 1976); (e) E. E. Nikitin, *Theory of Elementary Atomic and Molecular Processes in Gases* (Clarendon, Oxford, 1974); (f) K. F. Herzfeld, in *Thermodynamics and Physics of Matter* (Princeton University Princeton, 1965).

[2]F. Legay, in *Chemical and Biochemical Applications of Lasers II*, edited by C. B. Moore (Academic, New York, 1977); D. J. Diestler, in *Potential Energy Surfaces*, edited by K. P. Lawley (Wiley, New York, 1980); D. W. Oxtoby, Adv. Chem. Phys. 47, 487 (1981).

[3]F. E. Bartoszek, D. M. Manos, and J. C. Polanyi, J. Chem. Phys. 69, 933 (1978); D. J. Douglas, J. C. Polanyi, and J. J. Sloan, *ibid.* 59, 6679 (1973).

[4]S. H. Northrup and J. T. Hynes, Chem. Phys. Lett. 54, 244 (1978).

[5]F. E. Hovis and C. B. Moore, J. Chem. Phys. 69, 4947 (1978); A. B. Horwitz and S. R. Leone, *ibid.* 69, 5319 (1978); E. Weitz and G. W. Flynn, *ibid.* 58, 2679 (1973).

[6]L. Landau and E. Teller, Phys. Z. Sowjetunion 10, 34 (1936).

[7](a) R. N. Schwartz, Z. I. Slawsky, and K. F. Herzfeld, J. Chem. Phys. 20, 1591 (1952); (b) R. D. Sharma and C. A. Brau, *ibid.* 50, 924 (1969).

[8](a) C. J. Dasch and C. B. Moore, J. Chem. Phys. 72, 4117 (1980); (b) R. S. Sheory, R. C. Slater, and G. W. Flynn, *ibid.* 68, 1058 (1978); (c) J. K. Lampert, G. M. Jursich, and F. F. Crim, Chem. Phys. Lett. 71, 258 (1980); (d) J. R. Airey and I. W. M. Smith, J. Chem. Phys. 57, 1669 (1973); (e) P. R. Poole and I. W. M. Smith, J. Chem. Soc. Faraday Trans. 2 73, 1434, 1447 (1977); (f) D. J. Douglas and C. B. Moore, J. Chem. Phys. 70, 1769 (1979); (g) F. Kaufman (private communication).

[9](a) J. C. Polanyi and J. J. Sloan, J. Chem. Phys. 57, 4988 (1972); (b) D. J. Bogan and D. W. Setser, *ibid.* 64, 586 (1976); (c) M. Braithewaite and I. W. M. Smith, J. Chem. Soc. Faraday Trans. 2 72, 288 (1975).

[10]G. Herzberg, *Spectra of Diatomic Molecules* (Van Nostrand–Reinhold, New York, 1950).

[11]A. N. Schweid and J. I. Steinfeld, J. Chem. Phys. 58, 844 (1973), and preceding papers in the series; J. I. Steinfeld, in *Molecular Spectroscopy: Modern Research*, edited by K. N. Rao and C. W. Mathews (Academic, New York, 1972), p. 223.

[12]C. Kittrell, E. Abramson, J. L. Kinsey, S. A. McDonald, D. E. Reisner, R. W. Field, and D. H. Katayama, J. Chem. Phys. 75, 2056 (1981).

[13](a) A. G. Clarke and G. Burns, J. Chem. Phys. 58, 1908 (1973). For an earlier one dimensional study of high temperature Br_2 relaxation, see E. B. Alterman and D. J. Wilson, *ibid.* 42, 1957 (1965). The latter authors note that Δv often exceeds ± 1; inspection of their data shows that $\Delta E/k_b T$ is small and energy transfer is inefficient; (b) W. H. Wong and G. Burns, *ibid.* 62, 1712 (1975); Proc. R. Soc. London Ser. A 341, 105 (1974); A. Gelb, R. Kapral, and G. Burns, J. Chem. Phys. 59, 2980 (1973).

[14]M. Rubinson, B. Garetz, and J. I. Steinfeld, J. Chem. Phys. 60, 3082 (1974).

[15]B. H. Mahan, J. Chem. Phys. 52, 5221 (1970).

[16]W. Forst, *Theory of Unimolecular Reactions* (Academic, New York, 1973); P. J. Robinson and K. A. Holbrook, *Unimolecular Reactions* (Wiley, New York, 1972).

[17](a) J. Troe, Annu. Rev. Phys. Chem. 29, 223 (1978); (b) J. C. Keck, Disc. Faraday Soc. 33, 173 (1967).

[18]S. H. Northrup and J. T. Hynes, J. Chem. Phys. 73, 2700 (1980); R. F. Grote and J. T. Hynes, *ibid.* 73, 2715 (1980).

[19]R. L. McKenzie, J. Chem. Phys. 63, 1655 (1975).

[20]K. P. Huber and G. Herzberg, *Constants of Diatomic Molecules* (Van Nostrand–Reinhold, New York, 1979).

[21]A. J. Stace and J. N. Murrell, Mol. Phys. 33, 1 (1977).

[22]R. L. McKenzie, J. Chem. Phys. 66, 1457 (1977).

[23]G. E. Forsythe, M. A. Malcolm, and C. B. Moler, *Computer Methods for Mathematical Computations* (Prentice-Hall, Englewood Cliffs, 1977).

[24]J. I. Steinfeld and A. N. Schweid, J. Chem. Phys. 53, 3304 (1970).

[25]S. W. Benson and G. C. Berend, J. Chem. Phys. 40, 1289 (1964).

[26](a) There are actually a number of contradictory expressions for $P_{v\to v-1}$ in the literature: Eq. 148 and its limit Eq. 153 in Ref. 1(a) are correct (except for mass factors [Ref. 15]). (b) The average energy change $\Delta E(v_0) = \hbar\omega[P_{v\to v+1} - P_{v\to v-1}]$ for given projectile velocity v_0 is always positive unless the velocity change during excitation and de-excitation collisions is accounted for [Ref. 1(a), Eq. (153); Ref. 1(c), p. 104]; this effect is also required by microscopic reversibility.

[27](a) D. J. Nesbitt and J. T. Hynes, Chem. Phys. Lett. 82, 252 (1981). The precise energy spacing $E(v)-E(v-1)$ is actually $\hbar$ times the average of the classical frequency at the two energies. The small numerical difference is unimportant for our purposes. (b) For low levels, rates can be readily related to ΔE [Ref. 1(a)]. At high levels, it is possible that rates can be extracted from a diffusion approach [J. C. Keck and G. Carrier, J. Chem. Phys. 43, 2284 (1965)], in which the energy diffusion coefficient is proportional to the mean square energy transfer, whose derivative is simply related to ΔE.

[28]J. F. Bott, J. Chem. Phys. 65, 4239 (1976); 70, 4129 (1979); G. M. Jursich and F. F. Crim, *ibid.* 74, 4455 (1981); R. L. McKenzie, *ibid.* 64, 1498 (1976).

[29]S. W. Benson, *The Foundations of Chemical Kinetics* (McGraw–Hill, New York, 1960), p. 163.

[30]S. W. Benson, G. C. Berend, and J. C. Wu, J. Chem. Phys. 38, 25 (1963).

[31]N. B. Slater, Proc. Leeds Phil. Lit. Soc. Sci. Ser. 8, 93 (1959).

[32]This result is also obtained by Benson *et al.* in Ref. 30. The exclusive use of Eq. (4.7) (i.e., without Eq. (4.8) in Refs. 25 and 30 to obtain average energy changes has been criticized [Ref. 1(a)].

[33]Equations (4.3)–(4.6) have no solutions for $E < 2\mu_{osc} v_0^2$; here the projectile always moves faster than the oscillator. It is only in this special regime that t_1 and t_2 span a full period and all oscillator phases are accessible.

[34]D. Bohm, *Quantum Theory* (Prentice–Hall, Englewood Cliffs, 1951), p. 282.

[35]D. J. Nesbitt and J. T. Hynes (to be submitted).

[36]D. J. Nesbitt and J. T. Hynes, J. Chem. Phys. (to be published).

[37]I. S. Gradshteyn and I. M. Ryzhik, *Table of Integrals, Series and Products* (Academic, New York, 1965), p. 84.

This article is copyrighted as indicated in the article. Reuse of AIP content is subject to the terms at: http://scitation.aip.org/termsconditions. Downloaded to IP: 35.8.11.3 On: Thu, 28 Jan 2016 10:16:35